PAIN®

Spinal cord interneurons expressing the gastrin-releasing peptide receptor convey itch through VGLUT2-mediated signaling

Bejan Aresh[a], Fabio B. Freitag[a], Sharn Perry[a], Edda Blümel[a], Joey Lau[b], Marina C.M. Franck[a], Malin C. Lagerström[a,*]

Abstract

Itch is a sensation that promotes the desire to scratch, which can be evoked by mechanical and chemical stimuli. In the spinal cord, neurons expressing the gastrin-releasing peptide receptor (GRPR) have been identified as specific mediators of itch. However, our understanding of the GRPR population in the spinal cord, and thus how these neurons exercise their functions, is limited. For this purpose, we constructed a Cre line designed to target the GRPR population of neurons (Grpr-Cre). Our analysis revealed that Grpr-Cre cells in the spinal cord are predominantly excitatory interneurons that are found in the dorsal lamina, especially in laminae II-IV. Application of the specific agonist gastrin-releasing peptide induced spike responses in 43.3% of the patched Grpr-Cre neurons, where the majority of the cells displayed a tonic firing property. Additionally, our analysis showed that the Grpr-Cre population expresses *Vglut2* mRNA, and mice ablated of *Vglut2* in Grpr-Cre cells (*Vglut2*-lox;Grpr-Cre mice) displayed less spontaneous itch and attenuated responses to both histaminergic and nonhistaminergic agents. We could also show that application of the itch-inducing peptide, natriuretic polypeptide B, induces calcium influx in a subpopulation of Grpr-Cre neurons. To summarize, our data indicate that the Grpr-Cre spinal cord neural population is composed of interneurons that use VGLUT2-mediated signaling for transmitting chemical and spontaneous itch stimuli to the next, currently unknown, neurons in the labeled line of itch.

Keywords: Itch, Gastrin-releasing peptide receptor population, Natriuretic polypeptide B, Spinal cord, Vesicular glutamate transporter 2, Neuronal networks, Labeled line of itch, Electrophysiology, Conditional knockout analysis, Tracing, Calcium imaging

1. Introduction

Itch, or pruritus, is a sensory modality that functions to remove potentially harmful pathogens. Although itch is most commonly associated with an acute state, for example, after a mosquito bite, itch can also exist in persistent forms in diseases, such as atopic dermatitis, urticaria, prurigo nodularis, and psoriasis. Pruritic substances are sensed by primary afferent neurons, or pruriceptors, which express a variety of receptors specifically devoted to the detection of endogenous and exogenous itch-inducing agents such as histamine or chloroquine.[16,26,28] The pruriceptive neurons are confined within the slowly conducting C-fibers and the thinly myelinated Aδ fibers, with their cell bodies in the dorsal root ganglia (DRG) and free nerve endings innervating the skin.[15,23,26] Once activated, pruriceptors convey the information to the spinal cord dorsal horn via neuropeptide natriuretic polypeptide B (NPPB)[17] and calcitonin gene–related peptide,[24] where the information is projected further via spinothalamic tract neurons to the brain for interpretation.[1] Although our knowledge about the initiation and transmission of pruritic signaling in the periphery has increased in the last couple of years, less is known about the central transmission of itch in the spinal cord.

The gastrin-releasing peptide receptor (GRPR) is a G-protein-coupled receptor expressed in the superficial layers of the dorsal horn.[10,30] *Grpr* knockout analysis has shown that GRPR is not involved in any pain modalities tested (thermal, mechanical, inflammatory, and neuropathic pain).[30] Intradermal injection of histamine and nonhistaminergic agents in *Grpr* knockout mice or gastrin-releasing peptide (GRP)-saporin–treated mice, however, led to a significant reduction in scratching, suggesting that GRPR and the GRPR-expressing neurons are mediators of both histamine-dependent and independent itch.[30,31] Still, little is known about the intrinsic properties of the spinal cord GRPR population. Here, we generated a Grpr-Cre mouse line using a bacterial artificial chromosome (BAC) cloning strategy to specifically label and manipulate the Grpr-Cre subpopulation of neurons, allowing us to reveal their inherent properties and to determine their position in the labeled line of itch.

2. Materials and methods

2.1. Generation of Grpr-Cre mice

The Grpr-Cre line was generated using a BAC cloning strategy based on http://recombineering.ncifcrf.gov/protocol/Protocol1_DY380.pdf. Briefly, the BAC RP23-395E7 (BACPAC Resources) consisting of a 189 kbp fragment, including the *Grpr* gene, was transferred to electrocompetent and recombination-induced EL250 cells by electroporation. These cells were plated on chloramphenicol (25 µg/mL; Fisher Scientific, Göteborg, Sweden) plates and positive colonies were controlled for BAC insertion using colony PCR and pulsed-field gel electrophoresis (CHEF Mapper; Bio-Rad, Solna, Sweden). A codon-improved Cre coding sequence together with an ampicillin cassette flanked by frt sites was inserted to replace exon 1 in the *Grpr* gene, and the cells were streaked onto plates with both chloramphenicol and ampicillin (100 µg/mL; Sigma, Stockholm, Sweden). Positive Cre-containing colonies were picked and treated with 10% arabinose (Sigma) to remove the ampicillin cassette. Finally, DNA from one of these colonies was purified using a Qiagen purification kit (large construct kit 10; Qiagen, Sollentuna, Sweden). The DNA sample was digested with NotI (Fermentas, Stockholm, Sweden) and run through a column (GE Healthcare, Uppsala, Sweden) to separate the vector from the desired DNA fragment. Thereafter, the purified DNA was sent for pronuclear injection at the Karolinska Center for Transgene Technologies (KCTT). Every subcloning stage was verified by PCR and pulsed-field gel electrophoresis. The primers used for wild type (*Grpr*) identification were 5′-cctggaagggattgtgagtt-3′ (forward) and 5′-cagcaag-tacctggctgaca-3′ (reverse) with a product size of 237 bp. The primers used for *Cre* identification were 5′-cctggaagggattgtgagtt-3′ (forward) and 5′-cgctgagataggtgcctcac-3′ (reverse) with a product size of 234 bp. Before verification with gel electrophoresis, the DNA plasmid was digested with the enzyme NotI and the following fragment sizes were obtained: for the *Grpr* gene 180.013 kbp and 8734 bp, for *Cre* 112.332 bp, 69.982 bp, and 8734 bp, and *Cre* after arabinose treatment 181.152 kbp and 8734 bp.

2.2. Animals

All animal procedures were approved by the local ethical committee in Uppsala and followed the Directive 2010/63/EU of the European Parliament and of the Council, The Swedish Animal Welfare Act (Djurskyddslagen: SFS 1988:534), The Swedish Animal Welfare Ordinance (Djurskyddsförordningen: SFS 1988:539), and the provisions regarding the use of animals for scientific purposes: DFS 2004: 15 and SJVFS 2012:26. Both female and male mice were used.

Founders carrying Grpr-Cre were crossed with the reporter line *tdTomato* (Gt(ROSA)26Sor^tm14(CAG-tdTomato)Hze; Allen Brain Institute), *Viaat-egfp* (GENSAT, MMRRC), or *Vglut2^f/f* mice.[33] Offspring were genotyped for the presence of the *Grpr-Cre* allele, the *tdTomato* allele, the *Viaat-egfp* allele, and the *Vglut2* allele. The following primers were used: *Grpr-Cre* 5′-gtgcaagctgaacaacagga-3′ (forward) and 5′-ccagcatccacattctcctt-3′ (reverse); *tdTomato* 5′-tgttcctgtacggcatgg-3′ (forward, mutant allele), 5′-ggcattaaagcagcgtatcc-3′ (reverse, mutant allele), 5′-aagggagctgcgtggagta-3′ (forward, wild type allele), 5′-ccgaaaatctgtgggaagtc-3′ (reverse, wild type allele); *Viaat-egfp* 5′-gacgtaaacggccacaagttc-3′ (forward, mutant allele), 5′-cttctcgttggggtctttgct-3′ (reverse, mutant allele); and *Vglut2^f/f* 5′-caggcaaaatctgtccacct-3′ (forward), 5′-agggtaggccaaaagcaatc-3′ (reverse). The Grpr-Cre allele was kept heterozygous.

2.3. Tissue preparation

Adult (>7 weeks) and P4 mice were anaesthetized by intraperitoneal injection of a mixture of 0.5 mg/mL ketamine hydrochloride (Ketaminol; Pfizer) and 0.5 mg/mL medetomidine hydrochloride (Domitor; Orion Pharma, Sollentuna, Sweden). The skin around the sternum as well as the diaphragm was cut and thereafter the veins below the liver and above the heart. Phosphate-buffered saline (Gibco Life Technologies) was pumped into the heart to remove the blood, before running 4% formaldehyde (HistoLab, Göteborg, Sweden) through the body. The brain (P4) and spinal cord (>7 weeks) were removed, postfixed in 4% formaldehyde, and run through a gradient of 10%, 20%, and 30% sucrose solutions (Sigma) before embedding in O.C.T compound (Sakura Finetek, Göteborg, Sweden) at −80°C. The spinal cord and brain were cut at a thickness of 14 and 16 µm, respectively, for immunohistochemical analysis.

2.4. Immunohistochemistry

Spinal cord and brain sections were rinsed in 1× tris-buffered saline (TBS), followed by incubation overnight at 4°C with primary antibodies diluted in blocking solution containing 0.5% gelatin (Bio-Rad) and 0.01% triton-X (Sigma-Aldrich) in 1×TBS. The following day, the sections were rinsed once again in 1×TBS before incubation at room temperature for 1.5 hours with the secondary antibodies. Before mounting the slides, the tissue was rinsed repeatedly in 1×TBS. The primary antibodies used were mouse monoclonal anti-NeuN 1:400 (Millipore, Solna, Sweden), chicken anti–green fluorescent protein 1:1000 (Abcam, Cambridge, United Kingdom), and rabbit anti-Pax2 1:200 (Biolegend, San Diego, CA). The secondary antibodies used were goat anti-chicken Alexa 647 1:200 (Invitrogen), donkey anti-mouse Alexa 488 1:400 (Invitrogen), and donkey anti-rabbit Alexa 647 1:400 (Invitrogen). IB4 was diluted 1:50 (conjugated to Alexa 647; Invitrogen) and 4′,6-diamidino-2-phenylindole (Sigma-life science) at 1:1000.

2.5. Tracing

Adult mice (>7 weeks) were placed in a plastic chamber receiving constant air flow of 430 mL/M and 3% to 4% isoflurane (Baxter, San Juan, Puerto Rico). Once anesthetized, the mouse was placed in a stereotaxic frame with a mask supplying air and isoflurane. Eye drops (Oftagel; Santen, Solna, Sweden) were applied to prevent dry eyes. Using a Q-tip, iodine (Jodopax; Pharmaxim) was applied onto the head of the mouse followed by a subcutaneous injection of 0.1 mL of the local anesthetic lidocaine (10 mg/mL; Apoteket). After 3 minutes, a scalpel was used to make a cut across the head exposing the skull. Hydrogen peroxide (30%) was applied onto the skull with a Q-tip, revealing the bregma and lambda. Once the coordinates were located for the lateral parabrachial nucleus (LPB) (AP: −5.20, ML: 1.20, DV: 3.50) and ventral posterolateral/medial thalamic nucleus (VPL/VPM) (AP: −1.94, ML: 1.70, DV: 3.75), a small hole was drilled and 100 nL of the retrograde tracer fluorogold (FG) (4%, FluoroChrome) was injected bilaterally. The needle was left at the injection site for 8 minutes before removal. The incision was sewed together using a suture (6 mm, Vicryl Rapide; Ethicon) and double knot after every stitch. The mouse was later returned to its home cage after receiving postoperative analgesic 0.03 mg/kg buprenorphine (Vetergesic; Orion Pharma). Animals were sacrificed 5 to 12 days postsurgery, and the tissue was handled according to procedures explained under tissue preparation. The brain was embedded in 4% agarose (Amresco, VWR, Stockholm, Sweden) and cut 60 µm thick on a vibratome (Leica Microsystems, Stockholm, Sweden), whereas the spinal cord was

embedded in O.C.T compound (Bio-Optica, Milano, Italy) and cut 16 to 30 μm thick for LPB and 30 to 60 μm for VPL/VPM.

2.6. Virus injection

Male and female Grpr-Cre mice aged 4 to 6 months were used for the virus injection experiments. The mice were anesthetized through inhalation of isoflurane (Baxter, induction at 4%, continuous anesthesia at 2%), and the body temperature was monitored and maintained at 36 to 37°C under the procedure using a heating pad (CMA). The fur on the back was shaved. The skin was cleaned with iodine (Jodopax vet; Pharmaxim, 20 mL/L in water) and a 1-cm incision was made along the midline above vertebrae T12-13 followed by a second incision that went through the connective tissue covering these 2 vertebrae. Next, cuts were made into the muscle on each side of T13 vertebra and a clamp was inserted to secure the spinal column. The ligamentum flavum connecting T12 with T13 was cut to reveal the spinal cord. Two injections of 500 nL virus each were made into the spinal cord parenchyma 0.4 mm right of the midline and 0.5 to 1 mm apart using a 10-μL Nanofil Hamilton syringe (WPI) with a 34G beveled needle (WPI) guided by a microsyringe pump controller (WPI) mounted on a stereotaxic frame. The tissue was kept moist throughout the procedure by continuous application of sterile saline (9 mg/mL; Fresenius Kabi) on the surgical area. AAV8/hSyn-DIO-mCherry (lot number AV4981F, titer: 6.1×10^{12} vg/mL) was purchased from UNC Vector core and AAV9/CAG-DIO-GCaMP6f-WPRE (lot number CS0722, titer 15.2×10^{12} vg/mL) from UPenn Vector core. Bupivacaine (Marcain; AstraZeneca, 2 mg/kg, subcutaneous) was administered as a local anesthetic at the site of surgery and buprenorphine (Vetergesic Vet; Orion Pharma, 0.1 mg/kg, subcutaneous) was used for postoperative analgesia. The animals were left 2 to 10 weeks after surgery before use in any experiments to achieve full recovery and efficient virus expression.

2.7. Single-cell PCR

Individual neurons for single-cell analysis were isolated through microdissection; here, adult (>7 weeks) tdTomato;Grpr-Cre–positive animals were euthanized with a of 0.5 mg/mL ketamine hydrochloride (Ketaminol; Pfizer) and 0.5 mg/mL medetomidine hydrochloride (Domitor; Orion Pharma). The mice were perfused, as described in section 2.3., with RNase free 1× phosphate-buffered saline, and the spinal cord was removed and immediately frozen on crushed dry ice. The frozen spinal cord was dry sectioned 10 μm thick and collected on membrane slides (Leica Microsystems). Single fluorescent tdTomato–positive cells from the most dorsal (predominately laminae I-III) spinal cord were picked using laser microdissection (Leica DM 600B) and collected in single tubes (VWR) containing cell collection solution (water, 0.1 M DTT [Invitrogen] and 20 U RNAse inhibitor [Fermentas]). The tubes were snap frozen on dry ice and stored in −80°C freezer until they were used for reverse transcription described below.

The single cells were thawed on ice for reverse transcription where 10 mM dNTPs and random primers were added directly to the tubes and incubated at 94°C for 5 minutes. The tubes were taken out immediately and incubated on ice for 5 minutes before 1× first-strand buffer (Invitrogen), 20 U RNAse inhibitor, and M-MLV (Invitrogen) were added followed by incubation at 37°C for 1 hour. To deactivate the enzyme, the reaction was incubated at 70°C for 15 minutes and was used in 2 rounds of PCR with 2 different primer pairs. In the first round of PCR, the following solutions were used: 10× buffer (Invitrogen), 1.5 mM MgCl

(Invitrogen), 0.5 U Platinum Taq (Invitrogen), and 0.4 μM of the primers. The same solutions were used in the second round (nested) of PCR together with 5 μL product from the first round of PCR, however with another primer pair. The protein β-actin was used as a positive control to ensure that the single tubes contained DNA. cDNA from the spinal cord and a water sample was included in each PCR to ensure that the protocol was optimal and that there were no contamination, respectively. The following primers were used in the first round of PCR: Grpr 5′-catctctagcctggctttgg -3′ (forward) and 5′-agatcttcat-cagggcatgg-3′ (reverse); Vglut2 5′-gccgctacatcatagccatc-3′ (forward) and 5′-gctctctccaatgctctcctc-3′ (reverse); β-actin 5′-ctctttccagccttccttctt-3′ (forward) and 5′-agtaatctccttctg-catcctgtc-3′ (reverse). In the nested PCR, the following primers were used: Grpr 5′-cagcaagtacctggctgaca-3′ (forward) and 5′-ggggttagtgctcttgaagg-3′ (reverse); Vglut2 5′-acatggtcaacaa-cagcactatc-3′ (forward) and 5′-ataagacaccagaagccagaaca-3′ (reverse). To ensure that the designed Grpr primers were specific, the Grpr product was sent for sequencing (Eurofins Genomics, Ebersberg, Germany) after the nested PCR.

2.8. Imaging

The images were obtained using a Mirax microscope (Pannoramic MIDI, 3D HISTECH; Hitachi, Tokyo, Japan) or an Olympus BX61WI microscope (Olympus, Lund, Sweden).

2.9. Electrophysiology and calcium imaging

Coronal 300 μm thick spinal cord slices from tdTomato;Grpr-Cre neonates (P4-P12) were prepared in a cold (4°C) sucrose-based oxygenated (95% O_2 and 5% CO_2) cutting solution composed of (mM): 2.49 KCl, 1.43 NaH_2PO_4, 26 $NaHCO_3$, 10 glucose, 252 sucrose, 1 $CaCl_2$, 4 $MgCl_2$. Alternatively, virus-injected Grpr-Cre adult mice (4-6 months old) were perfused and their spinal cord dissected and sliced in cold NMDG-HEPES–based recovery solution composed of (mM): 93 N-methyl-D-glucamine, 2.50 KCl, 1.20 NaH_2PO_4, 30 $NaHCO_3$, 20 HEPES, 25 Glucose, 5 sodium ascorbate, 2 thiourea, 3 sodium pyruvate, 10 $MgSO_4.7H_2O$, 0.5 $CaCl_2.2H_2O$. Thereafter, the slices were incubated at room temperature for 1 hour in a bubbling (with 95% O_2 and 5% CO_2) chamber containing normal artificial cerebrospinal fluid (mM): 126 NaCl, 2.5 KCl, 1.25 NaH_2PO_4, 26 $NaHCO_3$, 10 glucose, 1.5 $CaCl_2$, 1.5 $MgCl_2$. The slices were then transferred to a recording chamber whereby Grpr-Cre neurons were identified using a 60× water-immersion objective (LUMPlan FI, 0.90 numerical aperture; Olympus) through either red fluorescent protein for patch clamp or green fluorescent protein for calcium imaging, visualized on a Zyla sCMOS camera (Andor Technology Ltd, Belfast, United Kingdom) connected to a green (550 nm) or blue (490 nm; CoolLED System, Andover, United Kingdom) fluorescent LED light source. Patch electrodes (6-12 MΩ) from borosilicate glass capillaries (GC150F-10 Harvard Apparatus) pulled on a PC-10 gravitational pipette puller (Narishige, Tokyo, Japan) contained a K^+-based internal solution (in mM): 120 K-gluconate, 40 HEPES, 1.02 $MgCl_2$, 2.17 MgATP, 0.34 NaGTP, with pH adjusted to 7.2 using 1 M KOH with an osmolarity of 266 mOsm/L. Liquid junction potential was corrected before each patched neuron.

Whole-cell patch-clamp recordings were made using a multiclamp 700B amplifier (Molecular Devices, Sunnyvale, CA) and digitalized with Digidata 1440A (Molecular Devices), low pass filtered at 10 kHz, digitized at 20 kHz, and acquired and analyzed in WinWCP software (Dr J. Dempster, University of Strathclyde,

Glasgow, United Kingdom), and MATLAB (MathWorks, Natick, MA). Grpr-Cre neurons were voltage clamped at −60 mV and those with a stable resting membrane potential (Vm) lower than −45 mV were included in analysis. Grpr-Cre neuronal firing was examined by current injections (0-50 pA, 1 second, 10 pA increments) in current clamp with a 3-second step interval to assure membrane potentials returned to baseline. Action potentials (APs) elicited from depolarizing current pulses (5 pA increments, 10 ms), from rest, were analyzed for AP threshold, noted as the point when the increase in membrane potential exceeds 20 mV/ms.

After established spike profile and AP threshold, a 20-minute free-run protocol was recorded for each cell and 300 nM of GRP (Phoenix Europe GmbH, Burlingame, CA) was added. The agonist reached the bath in the recording chamber two and a half minutes of baseline and washed in for a total of 5 minutes. Subthreshold depolarization and induced spike activity were then analyzed.

Calcium-imaging responses from Grpr-Cre AAV9/CAG-DIO-GCaMP6–infected neurons to bath-applied NPPB (40 nM; Phoenix Europe GmbH) were recorded through a blue LED excitation light, and signals were acquired in a frame rate of 2 Hz. Each experiment consisted of 1.5 minutes of baseline followed by NPPB perfusion for a total of 5-minute recordings. Data presented here show relative change in the fluorescence signal from a region of interest. $\Delta F/F$ was calculated based on the mean value from the first 50 seconds of baseline.

2.10. Behavior

All behavior analyses were performed in a controlled environment at 20 to 24°C, 45% to 65% humidity, and 12-hour day/night cycle. The observers were blind to the genotype.

2.10.1. Spontaneous itch

The mice were placed in a transparent cage with bedding and recorded with a digital camera for 30 minutes. The scratching episodes were scored using the software AniTracker v1.0, and the results were displayed as the mean number of scratching episodes per group in 30 minutes.

2.10.2. Chemically induced itch

Adult (>7 weeks) $Vglut2\text{-}lox^{f/f}$;Grpr-Cre$^{tg/wt}$ (conditional knock-outs) and $Vglut2\text{-}lox^{f/f}$;Grpr-Cre$^{wt/wt}$ (controls) littermates were injected intradermally in the nape of the neck with 50 μL saline (9 mg/mL; Apoteket), placed in a transparent cage with bedding, and recorded for 1 hour. The subsequent day, the same animals were injected with 50 μL of compound 48/80 (10 μg; Sigma) or chloroquine (10 mM; Sigma) and recorded for another hour. The amount of scratching episodes was scored using the software AniTracker v1.0, and the data were presented as the mean number of scratching episodes for each group in 1 hour.

2.11. Pain

2.11.1. Von Frey

The mice were placed in transparent plastic chambers that were placed on an elevated metallic mesh floor for 90 minutes before the initiation of the experiment (acclimatization). Von Frey filaments (Scientific Marketing Associates) were applied on the planar surface of the hind paw of each mouse according to the Chaplain up–down paradigm.[5] A lift of the treated paw was considered a reaction to the applied filament and a thinner filament was applied subsequently, while a lack of reaction resulted in application of a thicker filament. Every observation started with 0.6 g filament and the experiment was ended once 6 measurements were obtained around the 50% threshold. The Dixon method[8] was used to calculate the 50% threshold.

2.11.2. Randall–Selitto

The mice were restrained in a transparent cylinder with their tail hanging out and left to acclimatize for 15 to 20 minutes. The Randall–Selitto arm[22] was placed on the tail and increasing pressure was applied until a reaction (tail flick) was observed and the machine was stopped. The test was repeated at least 3 times with 10 to 15 minutes between each test. The cutoff weight was 500 g, and the results were expressed as mean withdrawal latency in grams for each animal.

2.11.3. Hargreaves

The mice were placed in transparent plastic chambers that were placed on top of a glass floor for 90 minutes until no exploratory behavior was observed. A thermal laser beam (IITC Life Science, Woodland Hills, CA) was directed towards their planar hind paws and the time until paw withdrawal was noted. The test had a cutoff time of 20 seconds and was repeated at least 3 times with 5 minutes between each observation. The result was presented as the mean withdrawal latency (s) for each animal and group.

2.11.4. Tail withdrawal test

The mice were restrained in a plastic cylinder and left to acclimatize for 15 to 20 minutes before the tail was dipped halfway into −15°C ethanol. The tail was removed when a tail flick was observed or the cutoff time of 30 seconds was reached. The test was repeated at least 3 times with 5 to 10 minutes between each test, and the results were displayed as the mean withdrawal latency (s) for each animal and group.

2.12. Statistics

Nonparametric calculations of P values between 2 groups were conducted using the Mann–Whitney 2-tailed test. Neuronal membrane potential, input resistance, and AP threshold are presented as mean and SE. The computer program Prism version 5.01 (GraphPad Software Inc, La Jolla, CA) was used for all statistical tests.

3. Results

3.1. Grpr-Cre–expressing neurons comprise the Grpr population

To investigate the role of spinal GRPR-expressing neurons in itch transmission, we constructed a Grpr-Cre line using BAC cloning (**Fig. 1**). The Cre sequence together with an ampicillin cassette surrounded by frt sites was inserted into the vector replacing exon 1 of the *Grpr* gene (**Fig. 1A**). Digestion with restriction enzymes and pulsed-field electrophoresis revealed successful electroporation with 2 bands sized 180 and 8.7 kb for the wild type allele, whereas 3 bands sized 112, 70, and 8.7 kb were obtained for the mutant allele (**Fig. 1B**). Two healthy and viable Grpr-Cre founders were generated through pronuclear injection. To visualize the expression of Grpr-Cre, the line was crossed with *ROSA26-loxP-STOP-loxP-tdTomato* mice (hereafter referred to as *tdTomato*), which labels all Cre-active
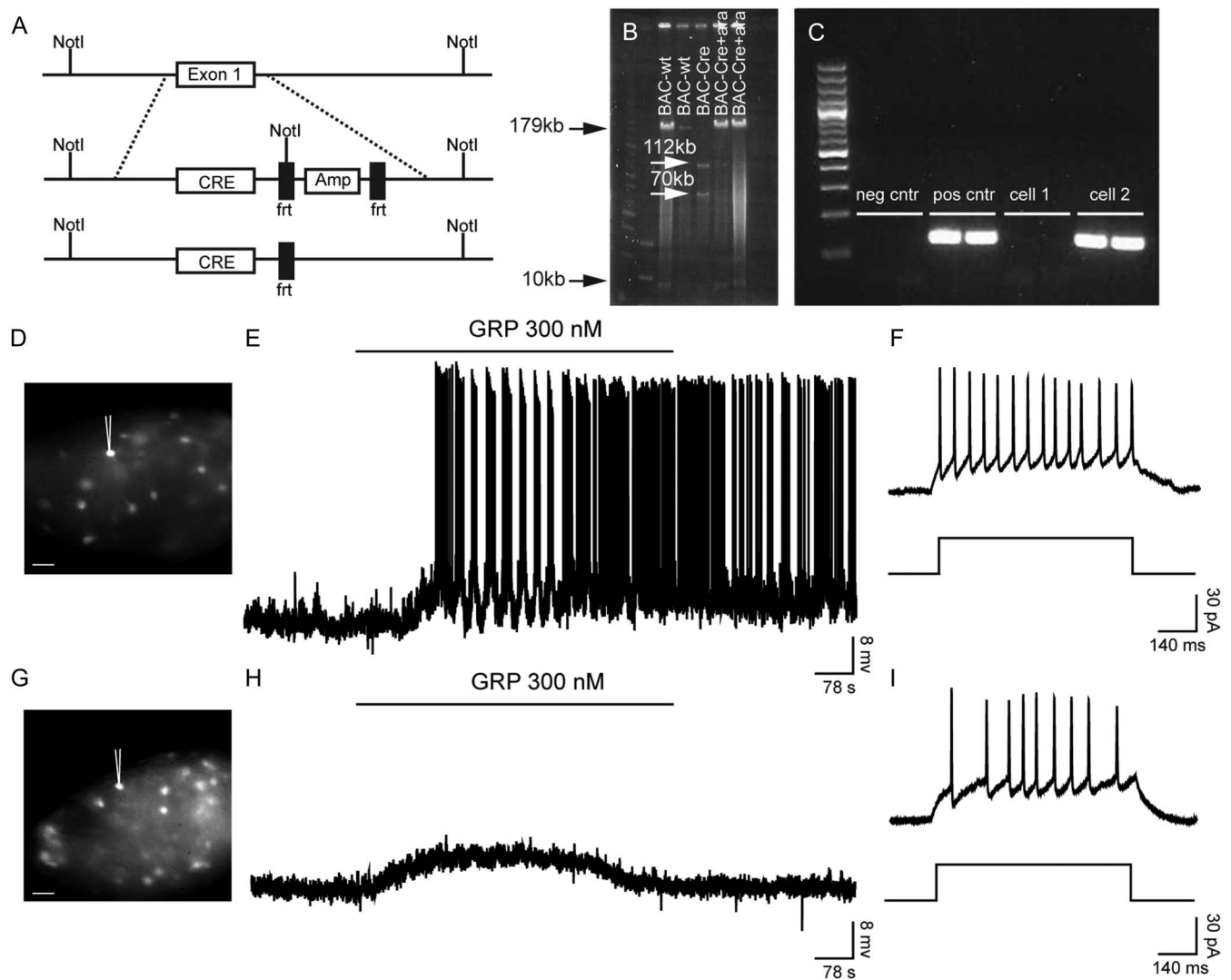
Figure 1. Construction of Grpr-Cre using BAC cloning. (A) Schematic overview of the generation of Grpr-Cre mice. The Cre sequence together with an ampicillin-resistance cassette flanked by 2 frt sequences was inserted through homologous recombination to replace exon 1 in the *Grpr* locus. Once inserted, the ampicillin-resistance gene was removed by the addition of arabinose, leaving only the Cre sequence under the influence of the *Grpr* promoter. (B) A pulsed-field gel electrophoresis image showing BAC-wt (180 bp and 8734 bp), BAC-Cre (112 kb, 70 kb, and 8734 bp), and arabinose-treated Cre (181 kb and 8734 bp). (C) Electrophoresis gel image from the single-cell analysis showing a positive and a negative cell for *Grpr*, ladder 100 bp. iCre (codon-improved Cre), frt (frt site), Amp (ampicillin-resistance gene). (D, E) Induction of action potentials in a *tdTomato*;Grpr-Cre cell when 300 nM gastrin-releasing peptide (GRP) was applied to the recording chamber. (F) Tonic spike profile exhibited by the recorded *tdTomato*;Grpr-Cre cell (D) when 30 pA current was applied. (G, H) A subthreshold depolarization response from a *tdTomato*;Grpr-Cre cell when 300 nM GRP was applied to the bath in the recording chamber. (I) A gap firing spike profile was exhibited by the recorded *tdTomato*;Grpr-Cre cell (G) when 30 pA of current was applied. Scale bars, 30 μm.

cells fluorescently red.[27] Single-cell analysis of *tdTomato*;Grpr-Cre cells gave a *Grpr*-specific band of 152 bp in 32% of Grpr-Cre cells (n = 86) (**Fig. 1C**), whereas none of the nonfluorescent cells expressed *Grpr* mRNA (n = 46), which indicates that the Grpr-Cre line includes the actual *Grpr* mRNA–expressing population.

To further evaluate GRPR expression in Grpr-Cre mice, the neuropeptide GRP (300 nM) was bath applied to patched *tdTomato*;Grpr-Cre cells located in the superficial layers of the dorsal horn spinal cord (**Fig. 1D–I**). Here, 43.3% (13/30) of the patched cells responded with APs of 0.5 ± 0.2 Hz during GRP application (**Fig. 1E**). Of those, 9 (69.2%) exhibited tonic (**Fig. 1F**), 2 (15.4%) adapting, and the other 2 (15.4%) delayed spike profile. The mean resting membrane potential was −56.8 ± 1.7 mV, input resistance 387.3 ± 30.9 MΩ, and AP threshold −30.6 ± 1.2 mV. In addition to the GRP spike-induced cells (43.3%), 16.7% (5/30) of the patched neurons responded with subthreshold depolarization ranging from 7 to 9 mV (**Fig. 1H**). Of these, 3 cells (60.0%) exhibited an adapting

profile, whereas the remaining 2 (40.0%) displayed a gap firing spike profile (**Fig. 1I**). Their resting membrane potential had a mean value of −57.10 ± 1.46 mV, the input resistance 407.00 ± 47.08 MΩ, and AP threshold −31.4 ± 1.6 mV (for a complementary electrophysiological analysis of the Grpr-Cre population, see Supplemental Fig. 1, available online at http://links.lww.com/PAIN/A389). Also, patch-clamp analysis of AAV8/hSyn-DIO-mCherry–infected Grpr-Cre neurons showed that out of 9 patched cells from 4 different animals (with mean values for resting membrane potential and input resistance of −58.29 ± 1.56 mV and 338.16 ± 8.46 MΩ, respectively), 2 responded with induced spikes (Supplemental Fig. 2, available online at http://links.lww.com/PAIN/A389), 5 with subthreshold depolarization of 5.00 ± 0.45 mV, and the remaining 2 with hyperpolarization of −12.00 ± 1.00 mV. Furthermore, input resistance decreased to 283.96 ± 6.16 MΩ after GRP bath application. These data further confirm that the Grpr-Cre population comprises GRPR/*Grpr*-expressing cells.

3.2. Grpr-Cre neurons in the spinal cord are mainly excitatory

To determine the expression of Grpr-Cre in the central and peripheral nervous system and the gross transmitter phenotype, *tdTomato*;Grpr-Cre mice were subsequently crossed with the *Viaat* (vesicular inhibitory amino acid transporter)-*egfp* line to visualize inhibitory neurons. The density of Grpr-Cre–expressing cells and the overlap with *Viaat-egfp* expression was graded as sporadic (+), intermediate (++), or dense (+++) for each evaluated brain structure, spinal cord segment, or peripheral structure analyzed. Grpr-Cre expression was identified in a number
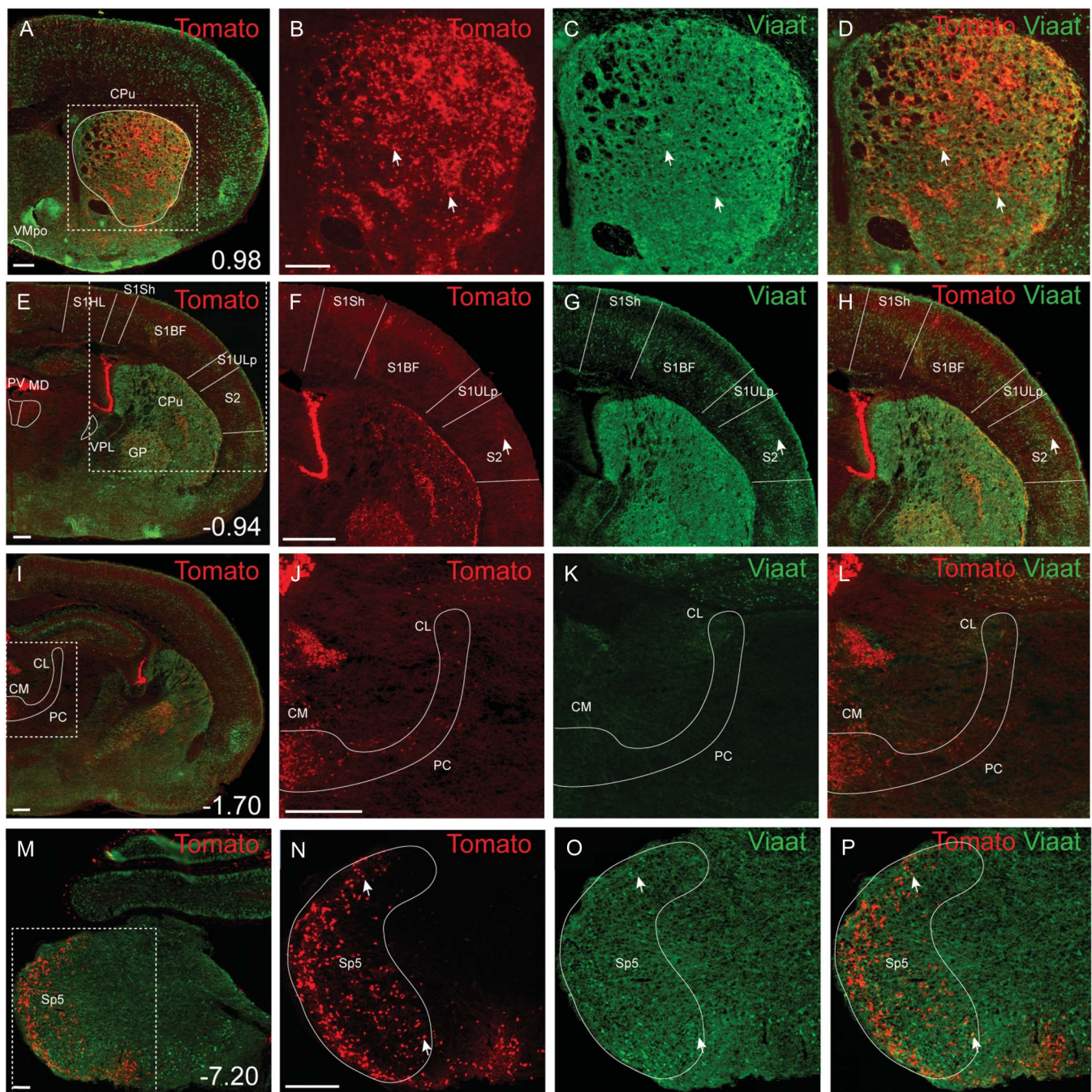

Figure 2. Expression of Grpr-Cre and *Viaat-egfp* in the brain. (A-P) Coronal section of a postnatal (P4) brain showing Grpr-Cre–expressing cells by the reporter line tdTomato indicated by red fluorescence (B, F, J, N) and *Viaat-egfp*–expressing neurons seen in green via the reporter *Viaat-egfp* (C, G, K, O). (A) Grpr-Cre activity was seen in certain brain regions, including the caudate putamen. (B-D) Enlargement of the caudate putamen. (E) Grpr-Cre activity was seen in the cortex. (F-H) Enlargement of the primary and secondary somatosensory cortices. (I) Grpr-Cre activity was seen in the central medial thalamic nuclei and paracentral thalamic nucleus. (J-L) Enlargement of the central medial thalamic nuclei and paracentral thalamic nucleus. (M) Grpr-Cre activity was seen in the spinal trigeminal nucleus. (N-P) Enlargement of the spinal trigeminal nucleus. Scale bars: 100 μm (A, E, I); 200 μm (B, M, N), and 500 μm (F, J). An antibody against green fluorescent protein was used to enhance detection. The arrows highlight examples of coexpression of green fluorescent protein and Grpr-Cre. CM, central medial thalamic nuclei; CL, centrolateral thalamic nuclei; CPu, caudate putamen; GP, globus pallidus; MD, mediodorsal thalamic nuclei; S1HL, primary somatosensory cortex, hindlimb region; S1Sh, primary somatosensory cortex, shoulder region; S1BF, primary somatosensory cortex, barrel field; S1ULp, primary somatosensory cortex, upper lip region; S2, secondary somatosensory cortex; Sp5, spinal trigeminal nucleus; PC, paracentral thalamic nucleus; PV, paraventricular thalamic nuclei; VPL, ventral posterolateral thalamic nuclei.

Table 1

tdTomato;Grpr-Cre and *Viaat-egfp* expression in P4 mouse brain.

Structure	Structure (full name)	Grpr-Cre	*Viaat-egfp*	Vglut2 in situ*
5N	Motor trigeminal nucleus	+	+	
10N	Dorsal motor nucleus of vagus	+		
AA	Anterior amygdaloid area	++		+
Acbc	Accumbens nucleus, core	+++		
AcbSh	Accumbens nucleus, shell	+++		
ACo	Anterior cortical amygdaloid area	+		+
AHA	Anterodorsal thalamic nucleus	+		
AHiAL	Amygdalohip area, antolateral	+		
AHiPM	Amygdalohippocampal area, posteromedial part	+	+	
AHP	Anterior hypothalamic area, posterior part	+		
AID	Agranular insular cortex, dorsal part	+		
AIP	Agranular insular cortex, posterior part	+		
AIV	Agranular insular cortex, ventral part	+	+	
AOD	Anterior olfactory area, dorsal part	+	+	
AOL	Anterior olfactory area, lateral part	+	+	
AOM	Anterior olfactory area medial part	+		
AOP	Anterior olfactory area posterior part	+		
AOV	Anterior olfactory area ventral part	+	+	
AP	Area postrema	+++		
APT	Anterior pretectal nucleus	+		+++
Arc	Arcuate hypothalamic nucleus	++		
ArcD	Arcuate hypothalamic nucleus, dorsal part	+++		
ArcL	Arcuate hypothalamic nucleus, lateral part	+++		
ArcM	Arcuate hypothalamic nucleus, medial part	+++		
ATg	Anterior tegmental nucleus	+	++	
Au1	Primary auditory cortex	+		
AuD	Secondary auditory cortex, dorsal	+	+	
AVPe	Anteroventral periventricular nucleus	+		+
AuV	Secondary auditory cortex, ventral area	+		
BMA	Basomedial amygdaloid nucleus, anterior part	++	+	+++
CA1	Field CA1 of the hippocampus	+	+	++
CA2	Field CA2 of the hippocampus	+	+	++
CA3	Field CA3 of the hippocampus	+	+	++
CeC	Central amygdaloid nucleus, capsular	++		
CeM	Central amygdaloid nucleus, medial division	++		
CEnt	Caudomedial entorhinal cortex	+		
Cerebellum		+++	+	
Cg 1	Cingulate cortex, area 1	+	+	
Cg2	Cingulate cortex, area 2	+	+	
Cl	Claustrum	+		
CIC	Central nucleus of the inferior colliculus	++		+++
CL	Centrolateral thalamic nucleus	+		
CM	Central medial thalamic nucleus	++		+++
CP	Cerebral peduncle	+++ projections		
CPu	Caudate putamen (striatum)	+++	+ projections	

Table 1 (*continued*)

Structure	Structure (full name)	Grpr-Cre	*Viaat-egfp*	Vglut2 in situ*
CxA	Cortex-amygdala transition zone	+	+	+
DC	Dorsal cochlear nucleus	++		
DCIC	Dorsal cortex of the inferior colliculus	++	+	+++
DEn	Dorsal endopiriform claustrum	+		
DEN	Dorsal endopiriform nucleus	+		
DG	Dentate gyrus	++	+	
DI	Dysgranular insular cortex	+ +	+	
DIEnt	Dorsal intermediate entorhinal cortex	+		
DLEnt	Dorsolateral entorhinal cortex	+	+	
DLO	Dorsolateral orbital cortex	+	+	
DLPAG	Dorsolateral periaqueductal gray	+	+	+++
DM	Dorsomedial hypothalamic nucleus	+++		+
DMC	Dorsomedial hypothalamic nucleus, compact part	+++		
DMPAG	Dorsomedial periaqueductal gray	+		+++
DMSp5	Dorsomedial spinal trigeminal nucleus	++		
DMTg	Dorsomedial tegmental area	+	+	
DP	Dorsal peduncular cortex	+	+	
DRD	Dorsal raphe nucleus, dorsal part	+		
DRL	Dorsal raphe nucleus, lateral part	+		
DRV	Dorsal raphe nucleus, ventral part	+		
DS	Dorsal subiculum	+	+	++
EAC	Extended amygdala, central part	+		
EAM	Extended amygdala, medial part	++		
ECIC	External cortex of the inferior colliculus	+	+	+++
Ect	Ectorhinal cortex	+	+	
EP	Entopeduncular cortex	+ projections	+ projections	+
Fr3	Frontal cortex, area 3	+		
FrA	Frontal association cortex	++	++	
Fu	Bed nucleus of the stria terminalis, fusiform part	+		
Gi	Gigantocellular reticular nucleus	+	+	
GI	Granular insular cortex	+	+	
GP	Globus pallidus	+++ projections	+ projections	
GrO	Granule cell layer of the olfactory bulb	+	+	
HDB	Nucleus of the horizontal limb of the diagonal band	+		++
IEn	Intermediate endopiriform claustrum	+		
IG	Indusium griseum	++		
IL	Infralimbic cortex	+	+	Projections
InG	Intermediate gray layer SC	++		+++
InWh	Intermediate white layer SC	+		+++
IOM	Inferior olive, medial nucleus	+	+	
IPACL	Interstitial nucleus of the posterior limb in the anterior commissure, lateral part	++		
IPACM	Interstitial nucleus of the posterior limb in the anterior commissure, medial part	++		
IPDM	Interpeduncular nucleus, dorsomedial subnucleus	+++		
IRt	Intermediate reticular nucleus	+		

Table 1 (*continued*)

Structure	Structure (full name)	Grpr-Cre	*Viaat-egfp*	Vglut2 in situ*
KF	Kolliker-Fuse nucleus	+		++
LA	Lateroanterior hypothalamic nucleus	+		+++
LAcbSh	Lateral accumbens shell	+		
LH	Lateral hypothalamic area	++	+	+
LHb	Lateral habenular nucleus, lateral	++		
LO	Lateral orbital cortex	++	+	
LPAG	Lateral periaqueductal gray	+		+++
LPBC	Lateral parabrachial nucleus, central part	++		++
LPGi	Lateral paragigantocellular nucleus	+		
LPMR	Lateral posterior thalamic nucleus, mediorostral	+		++
LPtA	Lateral parietal association cortex	+		
LSI	Lateral septal nucleus, intermediate part	++	+	
M1	Primary motor cortex	+	+	
M2	Secondary motor cortex	+	+	
mcp	Middle cerebellar peduncle	+	+	
MD	Mediodorsal thalamic nucleus	+++		+++
MdD	Medullary reticular nucleus, dorsal part	++		
MdV	Medullary reticular nucleus, ventral part	+	+	
ME	Median eminence	++		
MeA	Medial amygdaloid nucleus, anterior part	++		
MeAV	Medial amygdaloid nucleus, anteroventral part	++		+++
MEnt	Medial entorhinal cortex	+	+	
MePD	Medial amygdaloid nucleus, posterodorsal	+		
MePV	Medial amygdaloid nucleus, posteroventral	++		+++
mfb	Medial forebrain bundle	++	+ projections	+
MiTg	Microcellular tegmental nucleus	+		+
ml	Medial lemniscus	+++		
ML	Mammillary nucleus, medial part	+		+++
MO	Medial orbital cortex	+	+	
MoDG	Molecular layer of the dentate gyrus	++	+	
MPA	Medial preoptic area	+	+	+
MPOL	Medial preoptic nucleus, lateral part	+		
MPOM	Medial preoptic nucleus, medial part	+	+	
MPtA	Medial parietal association cortex	+		
MVePC	Medial vestibular nucleus, magnocellular part	+	+	
Op	Optic nerve layer of the superior colliculus	+		++
OT	Nucleus of the optic tract	++		+
P1Rt	p1 periaqueductal gray	+		
PaAP	Paraventricular hypothalamic nucleus, anterior parvocellular part	++		+
PaMP	Paraventricular hypothalamic nucleus, medial parvocellular part	+++		
PaLM	Paraventricular hypothalamic nucleus, lateral magnocellular part	+++		
PaPo	Paraventricular hypothalamic nucleus, posterior part	++		++
PaS	Parasubiculum	+	+	

Table 1 (*continued*)

Structure	Structure (full name)	Grpr-Cre	*Viaat-egfp*	Vglut2 in situ*
PC	Paracentral thalamic nucleus	+		+++
PCRtA	Parvocellular reticular nucleus, alpha part	+		+
PDR	Posterodorsal raphe nucleus	+		
Pe	Periventricular hypothalamic nucleus	+		
PH	Posterior hypothalamic nucleus	+		++
PHD	Posterior hypothalamic nucleus, dorsal part	+		
Pir	Piriform cortex	+	+	+
PL	Paralemniscal nucleus	+	+ projections	++
PLCo	Posterolateral cortical amygdala	+++	+	
PLH	Peduncular part of lateral hypothalamus	+++ projections		++
PMCo	Posteromedial cortical amygdaloid area	+		+++
Pn	Pontine nuclei	+		++
PnC	Pontine reticular nucleus, caudal part	+	+	+
PnO	Pontine reticular nucleus, oral part	+	+	++
PoDG	Polymorph layer of the dentate gyrus	++	+	
Post	Postsubiculum	+	+	
Pr5	Principal sensory trigeminal nucleus	+ projections		++
Pr5VL	Principal sensory trigeminal nucleus, ventrolateral part	+	+	+
PrCnF	Precuneiform area	++	+	+
PRh	Perirhinal cortex	+		
PrL	Prelimbic cortex	+	+	Projections
PrS	Presubiculum	+	+	
Ps	Parastrial nucleus	+		
PSTh	Parasubthalamic nucleus	++		+++
PV	Paraventricular thalamic nucleus	+++		+++
RAPir	Rostal amygdalopiriform	++		
RChL	Retrochiasmatic area	++		
RML	Retromammillary nucleus	++		+++
RSA	Retrosplenial agranular cortex	++		
RSD	Retrosplenial dysgranular cortex	+	+	
RSGa	Retrosplenial granular cortex, a region	+	+	
RSGb	Retrosplenial granular cortex, b region	+	+	
RSGc	Retrosplenial granular cortex, c region	+	+	
Rt	Reticular nucleus (prethalamus)	+++		
RTg	Reticulotegmental nucleus of the pons	++		
S1	Primary somatosensory cortex	+		
S1BF	Primary somatosensory cortex, barrel region	++	+	
S1DZ	Primary somatosensory cortex, forelimb region	+	+	
S1FL	Primary somatosensory cortex, forelimb region	+	+	
S1HL	Primary somatosensory cortex, hindlimb region	+	+	
S1J	Primary somatosensory cortex, jaw region	+	+	
S1Sh	Primary somatosensory cortex, shoulder region	+	+	
S1Tr	Primary somatosensory cortex, trunk region	+	+	
S1ULp	Primary somatosensory cortex, upper lip region	+	+	
S2	Secondary somatosensory cortex	+	+	

Table 1 (*continued*)

Structure	Structure (full name)	Grpr-Cre	*Viaat-egfp*	Vglut2 in situ*
SFi	Septofimbrial nucleus	+		
Shy	Septohypothalamic nucleus	+		++
SNR	Substantia nigra	+++ projections	+++ projections	
SolDL	Solitary nucleus, dorsolateral part	++		
SolDM	Solitary nucleus, dorsomedial part	++		
SolM	Solitary nucleus, medial part	++		
SolVL	Solitary nucleus, ventrolateral part	++		
Sp5	Spinal trigeminal tract	++ projections	+	
Sp5C	Spinal trigeminal nucleus, caudal part	+++	+	
Sp5I	Spinal trigeminal nucleus, interpolar part	+++	+	
SpVe	Spinal vestibular nucleus	++	+	
St	Stria terminalis	++		
ST	Bed nucleus of the stria terminalis	++		
STLD	Bed nucleus of the stria terminalis, lateral division, dorsal part	++		
STLJ	Bed nucleus of the stria terminalis, lateral division, juxtacapsular part	++		
STLP	Bed nucleus of the stria terminalis, lateral division, posterior part	+++		
STLV	Bed nucleus of the stria terminalis, lateral division, ventral part	+	+	
STMA	Bed nucleus of the stria terminalis, medial division, anterior part	++		
STMAL	Bed nucleus of the stria terminalis, medial division, anterolateral part	+++		
STML	Bed nucleus of the stria terminalis, medial division, posterolateral part	++		
STr	Subiculum, transition area	+		
SuG	Superficial gray layer of the superior colliculus	+	+	++
SubCD	Subcoeruleus nucleus, dorsal part	+	+	
SubB	Subbrachial nucleus	+	+	
SuVe	Superior vestibular nucleus	+		
TeA	Temporal association cortex	+	+	
tfp	Transverse fibers of pons	+++		
Tu	Olfactory tubercle	+++	+	
TuLH	Tuberal region of lateral hypothalamus	+		+
V1	Primary visual cortex	+	+	
V1B	Primary visual cortex, binocular area	+	+	
V1M	Primary visual cortex, monocular area	+	+	
V2L	Secondary visual cortex, lateral area	+	+	
V2ML	Secondary visual cortex, mediolateral	+	+	
V2MM	Secondary visual cortex, mediomedial	+	+	
VCA	Ventral cochlear nucleus, anterior part	++	+	++
VCP	Ventral cochlear nucleus, posterior part	++		
VEN	Ventral endopiriform nucleus	+		+
VIEnt	Ventral intermediate entorhinal cortex	+	+	
VLL			Projections	
VMHC	Ventromedial hypothalamic nucleus, central	++		++

Structure	Structure (full name)	Grpr-Cre	Viaat-egfp	Vglut2 in situ*
VMHDM	Ventromedial hypothalamic nucleus, dorsomedial part	++		+++
VMH	Ventromedial hypothalamic nucleus	+		++
VMHVL	Ventromedial hypothalamic nucleus, ventrolateral part	++		+++
VLPAG	Ventrolateral periaqueductal gray	+	+	+++
VLPO	Ventrolateral preoptic nucleus	+		
VP	Ventral pallidum	+++ projections		++
VTT	Ventral tenia tecta	+	+	

Grpr-Cre expression and overlap with the vesicular inhibitory amino acid transporter (Viaat) visualized using a transgenic line (forth panel), and with vesicular glutamate transporter 2 (Vglut2) mRNA (fifth panel)[34] in different brain nuclei. The expression and overlap was ranked either + sporadic, ++ intermediate, or +++ dense.
* Mackenzie et al., 2009, J Neurosci.

of nuclei throughout the brain (**Fig. 2**, **Table 1**). Particularly, dense Grpr-Cre expression was found in the caudate putamen (**Fig. 2A–D**) and globus pallidus (**Table 1**, **Fig. 2E–H**), where a majority of the cells in the caudate putamen overlapped with *Viaat-egfp* (**Fig. 2B–D**). Intermediate-to-sporadic Grpr-Cre expression was seen in both primary and secondary somatosensory cortices, predominantly in layer 2 and sporadically in layers 1 and 3 (**Fig. 2E–H**). A few of these cells overlapped with *Viaat-egfp*, which was expressed throughout the primary and secondary somatosensory cortices with the highest expression in layers 3 and 4 (**Fig. 2F–H**). Dense expression was seen in several thalamic structures, including paraventricular thalamic nuclei, mediodorsal thalamic nuclei, and central medial thalamic nuclei, whereas the expression was sporadic in paracentral thalamic nucleus and centrolateral thalamic nucleus (**Fig. 2E, I–L**). None of the Grpr-Cre–expressing nuclei in the thalamic region overlap with *Viaat-egfp*, which indicate that most Grpr-Cre–expressing nuclei in the thalamus are excitatory (**Fig. 2E, I–L**). This was further supported by a comparative *Vglut2* analysis, where dense expression of the transporter was visible in the above-mentioned thalamic structures (**Table 1**).[34] Grpr-Cre expression was also dense in the spinal trigeminal nucleus, which overlapped sporadic with *Viaat-egfp* (**Fig. 2M–P**). Besides the thalamus, several other itch-processing nuclei[19] showed the expression of Grpr-Cre, including the periaqueductal gray and parabrachial nucleus. Here, sporadic expression of Grpr-Cre was evident in the dorsolateral, lateral periaqueductal gray and ventrolateral periaqueductal gray (**Table 1**), whereas the expression was intermediate in the LPB (**Table 1**).

In the spinal cord, an intermediate number of Grpr-Cre–positive cells were found within laminae II, III, and IV, whereas sporadic expression could be detected in lamina I and deeper lamina (**Fig. 3A–C**). Inner lamina II was detected using the marker IB4. To determine whether Grpr-Cre cells were neurons or glial cells, overlap with the pan-neuronal marker NeuN was analyzed. Our analysis revealed that 97% of Grpr-Cre cells coexpressed NeuN (298 of 307) (**Fig. 3D–F**), indicating that Grpr-Cre cells are neurons. Concurrently, in laminae I-VI, only 11% of the Grpr-Cre–active neurons showed immunoreactivity towards *Viaat-egfp* (18 of 162) (**Fig. 3G–I**) and 6% with Pax2, a transcription factor that is required for the expression of GABAergic neurons during development[6] (10 of 183) (**Fig. 3J–L**). These results imply that Grpr-Cre neurons in the spinal cord are predominately excitatory. Expression of Grpr-Cre in the DRG was also analyzed to assess whether the population was restricted to the central nervous system or if Grpr-Cre was also active in the periphery. On average, only 4 Grpr-Cre neurons were located/DRG section (28 sections) (Supplemental Fig. 3, available

online at http://links.lww.com/PAIN/A389). Thus, Grpr-Cre activity is mainly confined to neurons within the central nervous system.

3.3. Spinal Grpr-Cre neurons represent predominately interneurons

To determine the termination of spinal cord Grpr-Cre neuron projections, tracing analyses were performed. The retrograde tracer FG was injected in LPB, VPL, and VPM of adult mice, and subsequently, traced projection neurons in the lumbar spinal cord were imaged (**Fig. 4**). Lateral parabrachial nucleus injections resulted in 137 FG-positive spinal cord cells, located in lamina I/lateral spinal nuclei (n = 96), lamina V/VII/VIII (n = 38), and lamina X (n = 3) (**Fig. 4A–I**), whereas injections targeting VPL/VPM resulted in 66 FG-positive cells located in laminae V (n = 25) and VI (n = 41) (**Fig. 4J–R**). None of the VPL/VPM-traced neurons overlapped with Grpr-Cre (**Fig. 4K–R**) and only 2 (lateral spinal nuclei, n = 2) of the LPB-traced neurons overlapped with Grpr-Cre (data not shown), which indicates that spinal Grpr-Cre neurons do not extend projections outside the spinal cord and, hence, are interneurons.

3.4. Grpr-Cre neurons use VGLUT2-mediated transmission to convey itch

Overlap analysis between *tdTomato*;Grpr-Cre and *Viaat-egfp* neurons in the spinal cord concluded that most Grpr-Cre neurons are excitatory (**Fig. 3G–I**). To challenge this hypothesis, we performed single-cell analysis of Grpr-Cre neurons, isolated through laser microdissection, in the dorsal spinal cord. The analysis showed that 51% of the analyzed Grpr-Cre population expressed *Vglut2* (vesicular glutamate transporter 2) mRNA (n = 99), whereas 63% of the *Grpr* mRNA–containing Grpr-Cre neurons expressed *Vglut2* mRNA (n = 24) (**Fig. 5A**); thus, corroborating our finding that *Grpr* mRNA–expressing Grpr-Cre neurons are mainly excitatory.

To investigate the role of VGLUT2-mediated transmission in Grpr-Cre neurons, we subsequently crossed the Grpr-Cre line with *Vglut2$^{f/f}$* mice. The resulting *Vglut2$^{f/f}$*;Grpr-Cre offspring were healthy and viable, but had a decreased body weight (17.7 ± 0.74 g vs 21.1 ± 0.91 g for littermate controls, $P = 1.4 \times 10^{-6}$). In sensory behavioral analysis, the *Vglut2$^{f/f}$*;Grpr-Cre mice responded normally to touch (**Fig. 5B**) and noxious thermal (**Fig. 5C–D**) stimuli, but showed an elevated response to noxious mechanical stimuli compared with littermate controls (119 ± 10.0 g vs 75 ± 8.2 g) (**Fig. 5E**). The insertion of Cre did not affect the sensory behavioral phenotype (**Fig. 5B–F**).
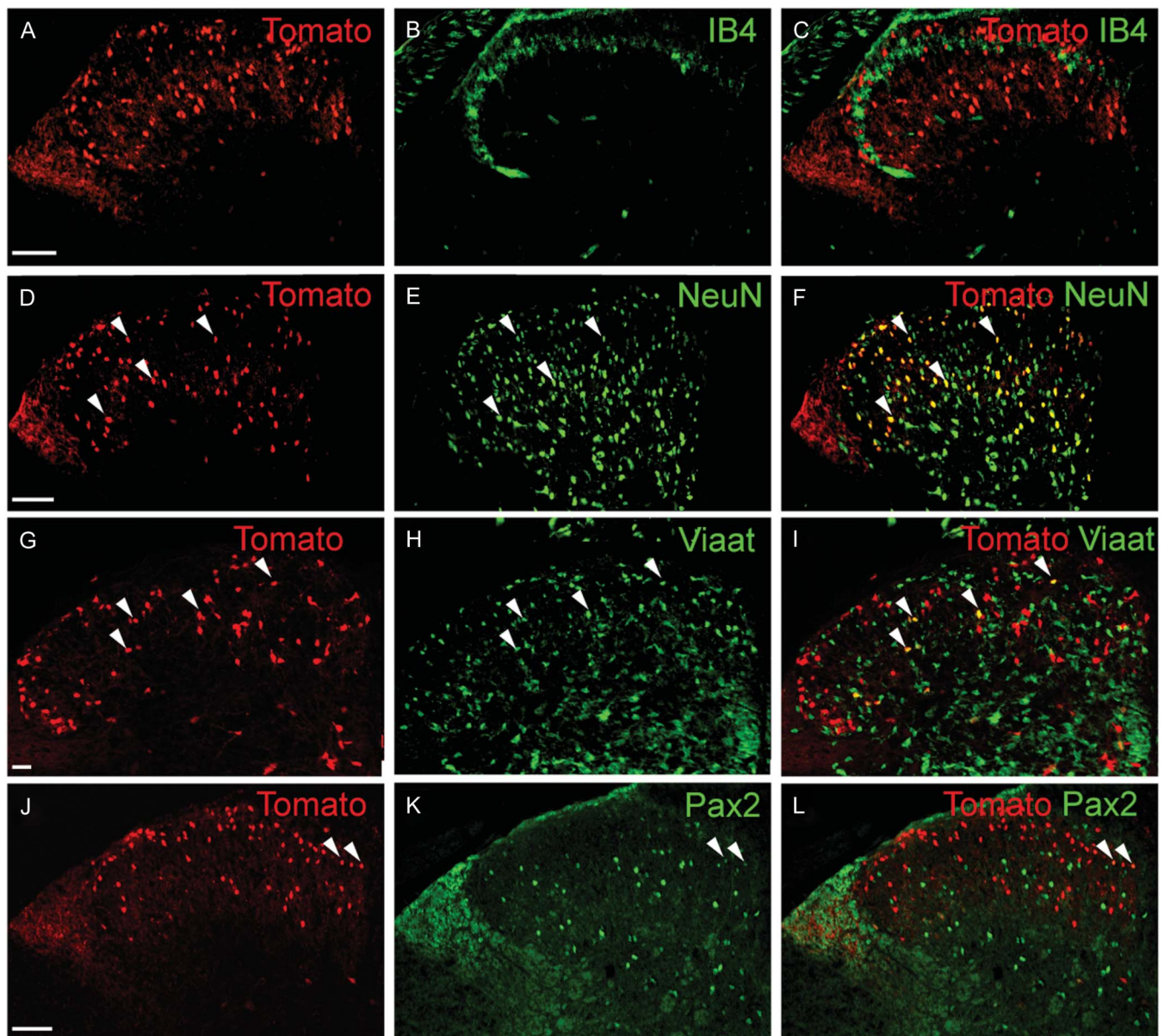
Figure 3. Grpr-Cre–expressing neurons in the spinal cord are primarily excitatory. Immunohistological analysis of transverse sections of *tdTomato*;Grpr-Cre mouse spinal cord. (A-C) Adult lumbar spinal cord stained for IB4 (green), which marks inner lamina II. (D-F) Labeling of adult lumbar spinal cord with NeuN (green) revealed that most (97%) Grpr-Cre–positive cells are NeuN positive. (G-I) Postnatal (P4) spinal cord showing Grpr-Cre (G) and *Viaat-egfp* (H) expression in the spinal cord dorsal horn. (J-L) Adult dorsal spinal cord labeled for Grpr-Cre and Pax2 (green). Scale bars, 100 μm. The arrowheads highlight examples of coexpression.

Interestingly, the spontaneous itch behavior of *Vglut2*$^{f/f}$;Grpr-Cre mice was attenuated compared with littermate controls (7 ± 3 scratch episodes per 30 minutes vs 14 ± 2 scratch episodes per 30 minutes) (**Fig. 5F**). A mild intradermal provocation, induced by an NaCl injection, resulted in an attenuated behavioral response in *Vglut2*$^{f/f}$;Grpr-Cre mice compared with littermate controls (20 ± 6 scratch episodes per hour vs 41 ± 8 scratch episodes per hour) (**Fig. 5G**). These results indicate that the Grpr-Cre population relays both spontaneous itch and the sensation of an isotonic injection via VGLUT2-mediated transmission. We also set out to investigate the role of VGLUT2-mediated transmission from Grpr-Cre neurons in chemically induced itch by introducing the pruritic agents compound 48/80 or chloroquine intradermally (**Fig. 5G**). The *Vglut2*$^{f/f}$;Grpr-Cre animals displayed reduced scratching behavior for both the histaminergic substance compound 48/80 (40 ± 8

scratch episodes per hour vs 222 ± 50 scratch episodes per hour) (**Fig. 5G**) and the nonhistaminergic substance chloroquine (143 ± 44 scratch episodes per hour vs 543 ± 110 scratch episodes per hour) (**Fig. 5G**), compared with control littermates. These behavioral results further supported the excitatory nature of the Grpr-Cre population and showed that Grpr-Cre interneurons convey both spontaneous and chemically induced itch via VGLUT2-mediated signaling.

To analyze the position and connectivity of the Grpr-Cre–expressing neurons in relation to known itch-related dorsal horn neuronal populations, the itch-associated neurotransmitter NPPB[17] was bath applied to spinal cord slices from Grpr-Cre neurons infected with AAV9/CAG-DIO-GCaMP6. From the 52 analyzed gfp-expressing cells, 12 (23.1%) responded with a mean 61.4% ± 13.9% increase in their fluorescence intensity level
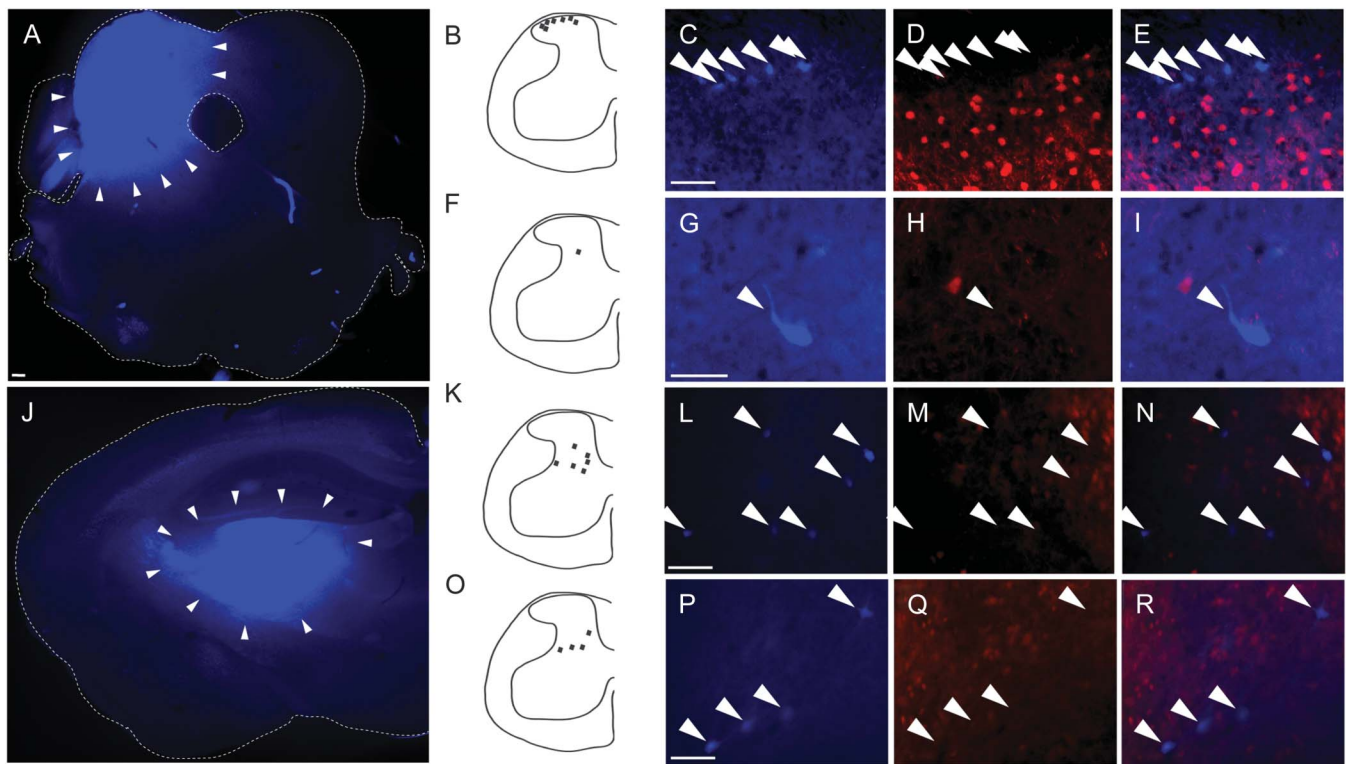
Figure 4. Grpr-Cre neurons are predominately interneurons. Images of the spinal cord after injection of tracer FG (blue) at LPB (A-I) and VPL/VPM (J-R). (A) Injection site of FG in LBP. Bregma −4.96 mm. (B-E) Examples of several projection neurons (blue, schematic in B) in lamina I where none of the traced neurons overlap with Grpr-Cre activity (red). (F-I) A representative traced neuron located in lamina V that did not overlap with Grpr-Cre activity. (J) Injection site of FG in VPL/VPM. Bregma −1.58 mm. K-R show several FG-positive neurons in laminae V and VI with no overlap with Grpr-Cre. Scale bar (A, J) 100 μm. Scale bar (C-E, G-I, L-N, P-R) 37 μm. FG, fluorogold; LPB, lateral parabrachial nucleus; VPL, ventral posterolateral nucleus of thalamus; VPM, ventral posteromedial nucleus of thalamus. The arrows denote the position of traced FG-positive neurons (projection neurons).

(**Fig. 5H and I**) (n = 2, 7 responding cells in the first animal and 5 responding cells in the second), suggesting a possible connectivity between natriuretic peptide receptor A (NPRA) and GRPR neurons.

4. Discussion

Here, we constructed a Cre line, driven by the *Grpr* promoter, to analyze *Grpr*-expressing neurons. Our single-cell and electrophysiological analyses confirmed that we target *Grpr*-expressing neurons, and our immunohistochemical and tracing analysis revealed that Grpr-Cre is predominantly expressed in excitatory interneurons in the dorsal horn of the spinal cord, particularly in laminae II, III, and IV. Grpr-Cre is almost absent in the DRG, whereas many structures in the brain, including the striatum, showed dense expression. The majority of Grpr-Cre–positive neurons in the brain overlapped with Viaat. Moreover, the behavioral analysis of *Vglut2*^f/f^; Grpr-Cre mice revealed that the Grpr-Cre population of interneurons is central for conveying itch and signals via VGLUT2-mediated transmission, as removal of *Vglut2* reduced both spontaneous and induced scratching behavior compared with littermate controls.

4.1. Grpr-Cre targets the Grpr population

Construction of a Cre line by BAC cloning uses random integration for insertion. To confirm the accuracy of our Cre insertion, we used several techniques where our single-cell analysis showed that 32% of the *tdTomato*;Grpr-Cre population

expressed *Grpr* mRNA and that all *Grpr*-expressing neurons were confined within the Grpr-Cre population. Moreover, our analysis revealed that 43.3% of *tdTomato*;Grpr-Cre cells responded to GRP application with induced APs, which matched our single-cell analysis of *Grpr* mRNA–expressing Grpr-Cre neurons. Additionally, 17% of the remaining patched cells responded with subthreshold depolarization, consistent with previous reports.[37] Interestingly, a high proportion (69%) of the spike responding cells were here classified as tonic neurons, a class that mainly includes excitatory interneurons.[25] Reporter lines often display a larger Cre population than actually present at the adult stage, due to transient expression during the development.[14,18] This is also evident from our analysis of *tdTomato*;Grpr-Cre neurons. To further analyze the active Grpr-Cre population at the adult stage, AAV8/hSyn-DIO-mCherry virus was injected in adult Grpr-Cre spinal cord tissue and all patched mCherry-positive neurons responded to GRP. Thus, we can conclude that *Grpr* mRNA–expressing neurons express Grpr-Cre and that Grpr-Cre neurons respond to the peptide GRP. Consequently, Grpr-Cre can be considered to target GRPR neurons.

4.2. Grpr-Cre neurons in the spinal cord dorsal horn are interneurons

The analysis of spinal GRPR neurons has so far been based on in situ hybridization,[30] a *Grpr-egfp* line[37] and real-time PCR,[10] which concluded that *Grpr* is expressed in the most superficial layers of the spinal cord, whilst being absent in the DRG.[10,17,30] This is consistent with our finding that Grpr-Cre–expressing cells
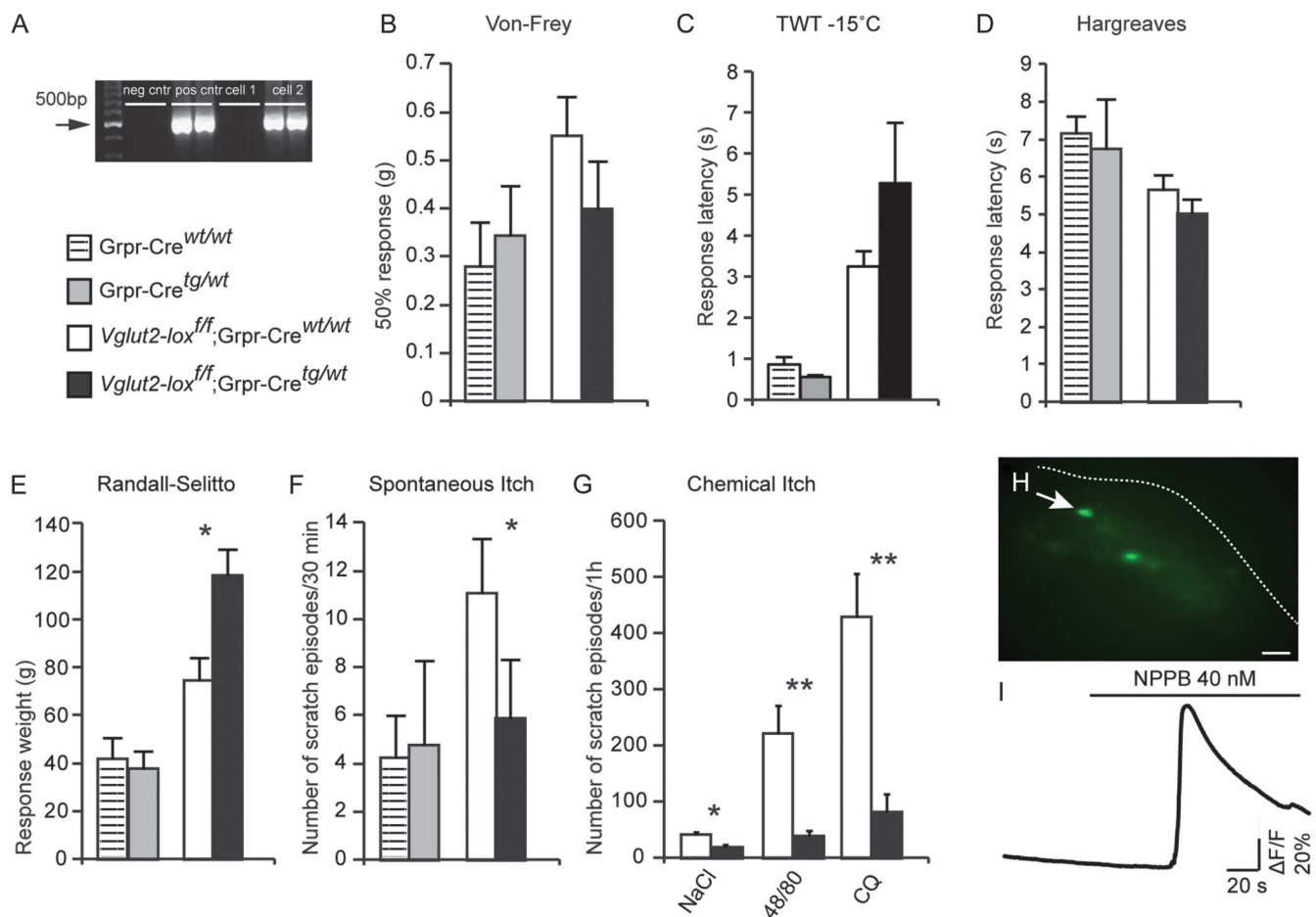
Figure 5. Grpr-Cre neurons signal using VGLUT2-mediated transmission. (A) Electrophoresis gel image showing a *Vglut2*-positive and negative cell, ladder 100 bp. (B-D) Grpr-Cre;*Vglut2*$^{f/f}$ responded normally to touch using von Frey filaments (n = 8, P = 0.20), to noxious cold and heat measured using tail withdrawal test (TWT, n = 9, P = 0.56) and Hargreaves test (n = 9, P = 0.34), respectively, compared with control littermates, (E) but displayed a significant difference when assessing noxious mechanical stimuli using Randall–Selitto (n = 7, P = 0.011). (F-G) Grpr-Cre;*Vglut2*$^{f/f}$ mice showed decreased spontaneous itch (n = 16, P = 0.044) behavior compared with littermate controls (F). Grpr-Cre;*Vglut2*$^{f/f}$ mice also displayed attenuated behavior after intradermal NaCl injection (n = 16, P = 0.018), attenuated itch behavior after compound 48/80 injection (10 μg, n = 7, P = 0.004) and chloroquine injection (10 mM, n = 9, P = 0.0012) (G). Insertion of the Cre cassette had no additional effects on touch (B), thermal pain (C-D), mechanical pain (E), or spontaneous itch (F) behavior. (H) Grpr-Cre neurons infected with AAV9/CAG-DiO-GCaMP6 in a 300 μM slice in the dorsal horn of a lumbar spinal cord section. (I) Representative trace of a Grpr-Cre–positive neuron responding to bath application of natriuretic polypeptide B (NPPB) 40 nM with an increase of 110% in its fluorescence. *P < 0.05, **P < 0.01, Mann–Whitney 2-tailed U test. Data described as mean ± SEM.

are located in the dorsal spinal cord; however, we also observe a few Grpr-Cre neurons in the DRG. This inconsistency can be due to the sensitivity of the *tdTomato* reporter, which enables detection of single Cre-active cells with high clarity or an incomplete overlap between Grpr-Cre and *Grpr* expression in adult. Tracing analysis with FG, injected into 2 major brain areas involved in itch processing[1]; the LPB[4,32] and VPL/VPM,[2] showed that only 2 of 203 traced projection neurons overlapped with *tdTomato*;Grpr-Cre–positive cells, which indicates that they represent interneurons. GRPR-positive neurons have previously been suggested to be separated from projection neurons based on the lack of overlap with NK1R,[38] a receptor expressed predominantly by projection neurons in lamina I of the dorsal horn of the spinal cord.[3,32,38] Our tracing data showed that Grpr-Cre neurons do not extend projections outside the spinal cord and, therefore, can be regarded as interneurons. In support, 9 of 13 of the GRP spike responding cells were here classified as tonic neurons, a class that has been reported as excitatory interneurons,[25] although tonic firing response neurons have also been correlated with inhibitory interneurons.[13,21,36]

4.3. Grpr-Cre is an excitatory itch-related population

Increasing evidence has emerged for the importance of excitatory neurons in a labeled line for itch.[11,29,35] Selective ablation of testicular orphan nuclear receptor 4 (TR4) in the central nervous system resulted in the loss of an excitatory interneuron population in the spinal cord dorsal horn. These transgenic animals displayed an absence of itch, an increased mechanical threshold and reduced pain behavior in response to noxious heat stimuli. Interestingly, a substantial (83%) loss of *Grpr* could be observed in the spinal cord of these TR4 conditional knockout mice.[35] As our single-cell data showed that 63% of *Grpr* mRNA/Grpr-Cre–expressing neurons also expresses *Vglut2*, it was of interest to investigate the outcome on sensory behavior of removing excitatory signaling, via VGLUT2, specifically from Grpr-Cre neurons by crossing Grpr-Cre with *Vglut2*-lox. The analysis revealed no differences between control and *Vglut2*-deficient mice in several pain tests except for an increased threshold for mechanical pain, which is in line with the mechanical pain phenotype observed in TR4 conditional knockout mice, which could suggest that an excitatory interneuron population confined

within TR4/Grpr-Cre/VGLUT2 neurons conveys mechanical pain. It has been shown that an excitatory population in lamina II, marked by the 2 neuropeptides; somatostatin and calretinin, is required for mechanical pain.[9,20] Possibly, a small subpopulation within Grpr-Cre that is confined to lamina II includes one or both of these neuropeptide populations and, hence, mediates the mechanical phenotype displayed by the *Vglut2-lox*;Grpr-Cre animals.

When assessing the itch phenotype in the *Vglut2*-deficient mice, decreased scratching episodes were observed compared with controls, for both the histaminergic and the nonhistaminergic substances. This supports previous data, inferring that GRPR expression defines an itch-specific population,[17,30,31] and we can now conclude that the itch transmission via GRPR neurons mainly relies on VGLUT2-mediated signaling. However, despite the evident support for glutamate-mediated itch transmission via Grpr-Cre neurons in the spinal cord, an additional central effect cannot be dismissed because Grpr-Cre is expressed in several brain nuclei and removing VGLUT2-mediated signaling could consequently affect these nuclei. Among these, thalamus, periaqueductal gray, and parabrachial nucleus are involved in itch processing (**Table 1**).[7,19]

Several itch-specific populations have been identified recently, adding to the increased evidence for a labeled line for itch.[17,31] Neurons expressing GRPR were the first population identified as a solely itch-transmitting population.[30,31] We propose that the Grpr population consists of excitatory interneurons that are activated by GRP and uses VGLUT2-mediated signaling to convey chemically induced pruritic transmission further. Whether Grpr-Cre neurons interact directly with projection neurons or excite a hitherto unknown itch-transmitting population needs further investigation. Previous data have placed the GRPR population as the tertiary line in itch transmission after itch-specific primary afferents expressing NPPB and interneurons expressing the NPRA and GRP.[17] Our analysis, using bath-applied NPPB and calcium imaging, shows that a potential subpopulation of Grpr-Cre neurons works downstream of NPRA neurons, as NPPB caused calcium influx in part of AAV9/CAG-DIO-GCaMP6–infected Grpr-Cre neurons. As NPRA and GRPR have been shown to not colocalize in the spinal cord,[12,17] these results suggest that the bath-applied NPPB was able to activate spinal NPRA neurons that possibly express GRP,[12,17] which subsequently led to activation of Grpr-Cre cells. Our findings, thus, allow us to place parts of the Grpr-Cre population downstream of NPRA neurons and upstream of itch-mediating projection neurons.

Conflict of interest statement

The authors have no conflicts of interest to declare.

Acknowledgements

Appendix A. Supplemental Digital Content

Supplemental Digital Content associated with this article can be found online at http://links.lww.com/PAIN/A389.

References

[1] Akiyama T, Curtis E, Nguyen T, Carstens MI, Carstens E. Anatomical evidence of pruriceptive trigeminothalamic and trigeminoparabrachial projection neurons in mice. J Comp Neurol 2016;524:244–56.

[2] Al-Khater KM, Kerr R, Todd AJ. A quantitative study of spinothalamic neurons in laminae I, III, and IV in lumbar and cervical segments of the rat spinal cord. J Comp Neurol 2008;511:1–18.

[3] Al-Khater KM, Todd AJ. Collateral projections of neurons in laminae I, III, and IV of rat spinal cord to thalamus, periaqueductal gray matter, and lateral parabrachial area. J Comp Neurol 2009;515:629–46.

[4] Bernard JF, Dallel R, Raboisson P, Villanueva L, Le Bars D. Organization of the efferent projections from the spinal cervical enlargement to the parabrachial area and periaqueductal gray: a PHA-L study in the rat. J Comp Neurol 1995;353:480–505.

[5] Chaplan SR, Bach FW, Pogrel JW, Chung JM, Yaksh TL. Quantitative assessment of tactile allodynia in the rat paw. J Neurosci Methods 1994;53:55–63.

[6] Cheng L, Arata A, Mizuguchi R, Qian Y, Karunaratne A, Gray PA, Arata S, Shirasawa S, Bouchard M, Luo P, Chen CL, Busslinger M, Goulding M, Onimaru H, Ma Q. Tlx3 and Tlx1 are post-mitotic selector genes determining glutamatergic over GABAergic cell fates. Nat Neurosci 2004;7:510–7.

[7] Davidson S, Zhang X, Khasabov SG, Moser HR, Honda CN, Simone DA, Giesler GJ Jr. Pruriceptive spinothalamic tract neurons: physiological properties and projection targets in the primate. J Neurophysiol 2012;108:1711–23.

[8] Dixon WJ. The up-and-down method for small samples. J Am Stat Assoc 1965;60:967–78.

[9] Duan B, Cheng L, Bourane S, Britz O, Padilla C, Garcia-Campmany L, Krashes M, Knowlton W, Velasquez T, Ren X, Ross SE, Lowell BB, Wang Y, Goulding M, Ma Q. Identification of spinal circuits transmitting and gating mechanical pain. Cell 2014;159:1417–32.

[10] Fleming MS, Ramos D, Han SB, Zhao J, Son YJ, Luo W. The majority of dorsal spinal cord gastrin releasing peptide is synthesized locally whereas neuromedin B is highly expressed in pain- and itch-sensing somatosensory neurons. Mol Pain 2012;8:1744–8069.

[11] Gutierrez-Mecinas M, Watanabe M, Todd AJ. Expression of gastrin-releasing peptide by excitatory interneurons in the mouse superficial dorsal horn. Mol Pain 2014;10:1744–8069.

[12] Kiguchi N, Sukhtankar DD, Ding H, Tanaka K, Kishioka S, Peters CM, Ko MC. Spinal functions of B-Type natriuretic peptide, gastrin-releasing peptide, and their cognate receptors for regulating itch in mice. J Pharmacol Exp Ther 2016;356:596–603.

[13] Labrakakis C, Lorenzo LE, Bories C, Ribeiro-da-Silva A, De Koninck Y. Inhibitory coupling between inhibitory interneurons in the spinal cord dorsal horn. Mol Pain 2009;5:24.

[14] Lagerstrom MC, Rogoz K, Abrahamsen B, Persson E, Reinius B, Nordenankar K, Olund C, Smith C, Mendez JA, Chen ZF, Wood JN, Wallen-Mackenzie A, Kullander K. VGLUT2-dependent sensory neurons in the TRPV1 population regulate pain and itch. Neuron 2010;68:529–42.

[15] LaMotte RH, Dong X, Ringkamp M. Sensory neurons and circuits mediating itch. Nat Rev Neurosci 2014;15:19–31.

[16] Liu Q, Tang Z, Surdenikova L, Kim S, Patel KN, Kim A, Ru F, Guan Y, Weng HJ, Geng Y, Undem BJ, Kollarik M, Chen ZF, Anderson DJ, Dong X. Sensory neuron-specific GPCR Mrgprs are itch receptors mediating chloroquine-induced pruritus. Cell 2009;139:1353–65.

[17] Mishra SK, Hoon MA. The cells and circuitry for itch responses in mice. Science 2013;340:968–71.

[18] Mishra SK, Tisel SM, Orestes P, Bhangoo SK, Hoon MA. TRPV1-lineage neurons are required for thermal sensation. EMBO J 2011;30:582–93.

[19] Papoiu AD, Coghill RC, Kraft RA, Wang H, Yosipovitch G. A tale of two itches. Common features and notable differences in brain activation evoked by cowhage and histamine induced itch. Neuroimage 2012;59:3611–23.

[20] Peirs C, Williams SP, Zhao X, Walsh CE, Gedeon JY, Cagle NE, Goldring AC, Hioki H, Liu Z, Marell PS, Seal RP. Dorsal horn circuits for persistent mechanical pain. Neuron 2015;87:797–812.

[21] Punnakkal P, von Schoultz C, Haenraets K, Wildner H, Zeilhofer HU. Morphological, biophysical and synaptic properties of glutamatergic neurons of the mouse spinal dorsal horn. J Physiol 2014;592:759–76.

[22] Randall LO, Selitto JJ. A method for measurement of analgesic activity on inflamed tissue. Arch Int Pharmacodyn Ther 1957;111: 409–19.

[23] Ringkamp M, Schepers RJ, Shimada SG, Johanek LM, Hartke TV, Borzan J, Shim B, LaMotte RH, Meyer RA. A role for nociceptive, myelinated nerve fibers in itch sensation. J Neurosci 2011;31:14841–9.

[24] Rogoz K, Andersen HH, Lagerstrom MC, Kullander K. Multimodal use of calcitonin gene-related peptide and substance P in itch and acute pain uncovered by the elimination of vesicular glutamate transporter 2 from transient receptor potential cation channel subfamily V member 1 neurons. J Neurosci 2014;34:14055–68.

[25] Santos SF, Rebelo S, Derkach VA, Safronov BV. Excitatory interneurons dominate sensory processing in the spinal substantia gelatinosa of rat. J Physiol 2007;581(pt 1):241–54.

[26] Schmelz M, Schmidt R, Bickel A, Handwerker HO, Torebjork HE. Specific C-receptors for itch in human skin. J Neurosci 1997;17:8003–8.

[27] Shaner NC, Campbell RE, Steinbach PA, Giepmans BN, Palmer AE, Tsien RY. Improved monomeric red, orange and yellow fluorescent proteins derived from Discosoma sp. red fluorescent protein. Nat Biotechnol 2004;22:1567–72.

[28] Sikand P, Dong X, LaMotte RH. BAM8-22 peptide produces itch and nociceptive sensations in humans independent of histamine release. J Neurosci 2011;31:7563–7.

[29] Solorzano C, Villafuerte D, Meda K, Cevikbas F, Braz J, Sharif-Naeini R, Juarez-Salinas D, Llewellyn-Smith IJ, Guan Z, Basbaum AI. Primary afferent and spinal cord expression of gastrin-releasing peptide: message, protein, and antibody concerns. J Neurosci 2015;35:648–57.

[30] Sun YG, Chen ZF. A gastrin-releasing peptide receptor mediates the itch sensation in the spinal cord. Nature 2007;448:700–3.

[31] Sun YG, Zhao ZQ, Meng XL, Yin J, Liu XY, Chen ZF. Cellular basis of itch sensation. Science 2009;325:1531–4.

[32] Todd AJ, McGill MM, Shehab SA. Neurokinin 1 receptor expression by neurons in laminae I, III and IV of the rat spinal dorsal horn that project to the brainstem. Eur J Neurosci 2000;12:689–700.

[33] Wallen-Mackenzie A, Gezelius H, Thoby-Brisson M, Nygard A, Enjin A, Fujiyama F, Fortin G, Kullander K. Vesicular glutamate transporter 2 is required for central respiratory rhythm generation but not for locomotor central pattern generation. J Neurosci 2006;26:12294–307.

[34] Wallen-Mackenzie A, Nordenankar K, Fejgin K, Lagerstrom MC, Emilsson L, Fredriksson R, Wass C, Andersson D, Egecioglu E, Andersson M, Strandberg J, Lindhe O, Schioth HB, Chergui K, Hanse E, Langstrom B, Fredriksson A, Svensson L, Roman E, Kullander K. Restricted cortical and amygdaloid removal of vesicular glutamate transporter 2 in preadolescent mice impacts dopaminergic activity and neuronal circuitry of higher brain function. J Neurosci 2009;29:2238–51.

[35] Wang X, Zhang J, Eberhart D, Urban R, Meda K, Solorzano C, Yamanaka H, Rice D, Basbaum AI. Excitatory superficial dorsal horn interneurons are functionally heterogeneous and required for the full behavioral expression of pain and itch. Neuron 2013;78:312–24.

[36] Yasaka T, Tiong SY, Hughes DI, Riddell JS, Todd AJ. Populations of inhibitory and excitatory interneurons in lamina II of the adult rat spinal dorsal horn revealed by a combined electrophysiological and anatomical approach. PAIN 2010;151:475–88.

[37] Zhao ZQ, Liu XY, Jeffry J, Karunarathne WK, Li JL, Munanairi A, Zhou XY, Li H, Sun YG, Wan L, Wu ZY, Kim S, Huo FQ, Mo P, Barry DM, Zhang CK, Kim JY, Gautam N, Renner KJ, Li YQ, Chen ZF. Descending control of itch transmission by the serotonergic system via 5-HT1A-facilitated GRP-GRPR signaling. Neuron 2014;84:821–34.

[38] Zhao ZQ, Wan L, Liu XY, Huo FQ, Li H, Barry DM, Krieger S, Kim S, Liu ZC, Xu J, Rogers BE, Li YQ, Chen ZF. Cross-inhibition of NMBR and GRPR signaling maintains normal histaminergic itch transmission. J Neurosci 2014;34:12402–14.